BMC Cancer

RESEARCH

Open Access

Validation of in vivo dose using EPID combined with fan-beam CT guidance in post-breast-conserving radiotherapy for early-stage breast cancer

Wanli Zhu[1†], Jia Fang[1†], Yi Zhang[1], Meiqin Chen[1], Hongzhi Zhang[1] and Shubo Ding[1*]

Abstract

Objective This study aimed to investigate the use of in vivo dose validation during post-breast-conserving radiation for early breast cancer, the impact of image guidance on validation outcomes, and the role of inter- and intra-fractional variations on dose distribution.

Methods Twenty-six patients undergoing post-breast-conserving radiotherapy for early-stage breast cancer were selected for in-treatment in vivo dose validation. The target area and organs at risk were re-defined using the image-guided images to quantitatively evaluate the impact of inter- and intra-fractional differences on the dose distribution. The retrospective analysis examined the in vivo dose validation outcomes.

Results The 3%3 mm/5%3 mm 2Dγ-pass (gamma pass) rates in the image-guided radiotherapy(IGRT) group were significantly higher than those in the non-IGRT(N-IGRT) group for both left and right breast cancer ($p < 0.05$). Furthermore, the 5%3 mm 2Dγ-pass rate of the fan-beam CT(FBCT) group was higher than that of the IGRT group and was statistically significant ($p < 0.05$). The target area parameters primary gross tumor volume (PGTV) D95, PGTV D2, planning target volume (PTV) D95, PTV D90, heart Dmean and V5, lung V5, and inter-fractional differences were statistically significant ($p < 0.05$) in patients with left breast cancer. The effects of intra-fractional differences on dose distribution were statistically significant except for cardiac Dmean ($p < 0.05$). Similarly, the dose distribution of measures including PGTV D95, PGTV D2, PTV D95, PTV D90, Heart Dmean, and Lung V5 was strongly impacted by inter-fractional variances in patients with right breast cancer. The influence of intra-fractional differences on dose distribution was statistically significant for all parameters ($p < 0.05$), and they were statistically significant ($p < 0.05$).

Conclusion When paired with fan-beam CT image guidance, electronic portal imaging device (EPID) in vivo dose validation provides a precise real-time dose delivery evaluation for patients undergoing radiation therapy for breast cancer.

[†]Wanli Zhu and Jia Fang contributed equally to this work.

*Correspondence:
Shubo Ding
jhyyys@163.com

Full list of author information is available at the end of the article

Keywords Breast cancer, Postoperative radiotherapy, Fan-beam CT-guided, In vivo dose verification, Electronic portal imaging device, Dose distribution

Introduction

Radiotherapy following breast-conserving surgery for early-stage breast cancer may enhance locoregional control, diminish the risk of tumor recurrence, and extend survival [1]. However, the potential for inadequate dosing to the targeted breast area and increased doses of normal tissues is a consequence of the inter- and intra-fractional differences that are present in the array of modern radiotherapy techniques available for breast cancer treatment [2, 3]. Inter-fractional variation occurs due to discrepancies between the patient's anatomical position during treatment and the intended position, affected by uncertainties in equipment settings (including rotation angles and cross-centering) and patient positioning factors (such as organ motion and patient movement). These discrepancies also result from difficulty accurately reproducing the patient's position during many therapy sessions. During a single treatment session, intra-fractional fluctuations mostly correspond to changes in the patient's posture or position by organ movement [4]. Disparities between the images used for treatment planning and those captured during treatment may result from these deviations, potentially leading to substantial discrepancies between the actual dose received by the patient and the dose prescribed by the treatment plan. The implementation of image-guided radiotherapy (IGRT) helps mitigate inter-fractional variation, with a study by Han et al. [5]. suggesting that daily image-guided fractions improve positioning accuracy and reduce dose discrepancies. While some studies [6, 7] have compared the positioning differences of breast cancer between treatment fractions, they did not consistently acquire anatomical information during irradiation. The study by Lee et al. [8] acquired in-treatment images to address intra-fractional dose variations from a dosimetric standpoint. However, the resulting dose data were derived based on a virtual plan rather than reflecting the actual dose received by the patient.

In vivo, dose validation evaluates the patient's actual absorbed dose by examining the transmitted dose and log data collected during therapy to confirm the precision of the administered dose [9, 10]. The study by Fang et al. [11] assessed the feasibility and efficacy of the approach in validating treatment progress, emphasizing pass rates. Their study concluded that substituting same-day fan-beam CT (FBCT) images for PlanCT images could enhance sensitivity and specificity, thus suggesting improved validity for in-process treatment validation.

Our research center intends to examine in vivo dosage outcomes in early breast cancer patients receiving breast-conserving radiation, employing image-guidance modalities and threshold criteria for validation. This study aims to investigate the therapeutic efficacy of in vivo dosage validation in breast-conserving radiation for early-stage breast cancer. Additionally, by combining in vivo dosage validation with image-guidance FBCT pictures, this study aims to investigate the effects of intra- and inter-fractional variations on patient dose distribution.

Materials and methods

Patients and positioning

A total of 26 patients with early breast cancer were randomly selected from those who underwent postoperative radiotherapy in our unit between May 2022 and March 2023. The average age of the patients was 54 years, with a median age of 50 years. The pathological stage was $T_{1-2}M_0N_0$, comprising 16 cases of left-sided breast cancer and 10 cases of right-sided breast cancer.

Inclusion criteria: (1) Breast cancer patients with tumor diameter less than 4 cm and no lymph node metastasis; (2) Age less than 65 years old; (3) Histological grade III or lymphatic vessel /Vascular invasion. Exclusion criteria: (1) Patients with an expected survival time less than 5 years; (2) Patients with contraindications to radiotherapy. A thermoplastic film (Colleridi, Guangzhou, China) and an integrated fixation plate (Macromedics, Sweden) were used to secure the patient's position. Discovery large-aperture CT (GE, USA) is used to collect free-breathing images of the patient and transmit the images to the uRT-TPOIS planning system (United Imaging Healthcare, China) to create radiotherapy plans and in vivo dose verification (referred to as in vivo) plans.

Linear accelerator and electronic portal imaging device

A cutting-edge radiation therapy tool, the uRT-linac 506c linear accelerator (Shanghai United Imaging Healthcare, China), integrates a 24-row diagnostic-grade fan-beam CT on the rear of a 6 MV X-ray linear accelerator. The head of the accelerator is equipped with 60 pairs of multileaf collimators, including 40 pairs in the center with 0.5 cm leaf thickness and 20 pairs on both sides with 1 cm leaf thickness, with a maximum field of 40 cm × 40 cm. sIMRT (static IMRT), dIMRT (dynamic IMRT), and uARC (volume-rotation-intensity-modulated radiation therapy) are supported by the device. Furthermore, the linear accelerator features an amorphous silicon electron portal imaging device (EPID). The EPID has a maximum frame rate of 15 frames per second (fps), an effective detection area of 40.96 cm × 40.96 cm, a source

image distance of 145 cm, and a resolution of 1024 × 1024 pixels in 1 × 1 binning mode. The pixels have a size of 0.4 mm and a spatial resolution of 0.27 mm at the isocenter plane. In addition to image guidance, the EPID device is equipped with in vivo dose verification 2D evaluation (hereafter referred to as in vivo 2D) and 3D reconstruction dose (hereafter referred to as in vivo 3D) evaluation functions.

In vivo dose verification function

(1) in vivo 2D function [12, 13]: Calculating transit images requires patient CT images and a Monte Carlo technique. Accurate modeling of the accelerator allows particle sampling to be done. Therefore, merging patient CT data helps monitor every particle precisely. The signal response of electrons and photons with different energies at different angles of incidence is obtained by accurate modeling of EPID [12–14], and the "pseudo-dose" image of particle deposition on a flat plate is calculated. Subsequently, particle scattering and energy deposition on the detector were modeled using the energy point spread function of the particles, resulting in the dose reference image for in vivo 2D. During treatment, radiation passes through the patient, depositing energy on the EPID is subsequently corrected for flat gain, geometry, and imperfections, resulting in a final measured image. A threshold is set to evaluate the expected and measured images, with conformity assessed through the γ-passing rate.

(2) in vivo 3D function: In the execution of the plan, details, including the positions of the multileaf collimator, collimator openings, and the actual beam intensity of the machine, are represented in the in vivo 2D measurement images. The in vivo 3D reconstruction algorithm model depends on the 2D images obtained during treatment. Flux maps used in dose calculation reconstruction are combined with patient CT data to get the reconstructed dose field for the patient. This process uses the fast Monte Carlo Dose Algorithm developed by United Imaging Healthcare, a Monte Carlo dosimetry algorithm [12, 14, 15], to calculate the patient's in vivo 3D reconstruction dose field.

Patient in vivo dose validation study workflow

Since May 2022, our unit has been officially conducting in vivo dosage validation of EPID for post-breast-conserving radiation in early breast cancer patients with the uRT-linac 506c (Jinhua Hospital associated with Zhejiang University School of Medicine Ethical Approval No. 48, 2022). The in vivo dosage validation method for the patient consists of three main phases: plan production, patient therapy, and 3D dose reconstruction (Fig. 1).

(1) Plan production: All target volumes and organs at risk (OARs) were scanned by CT series using the uRT-TPOIS planning system of United Imaging (Shanghai United Imaging, China. Version: R001) according to the Danish Cancer Breast Cancer Collaborative Group (DBCG) atlas [16]

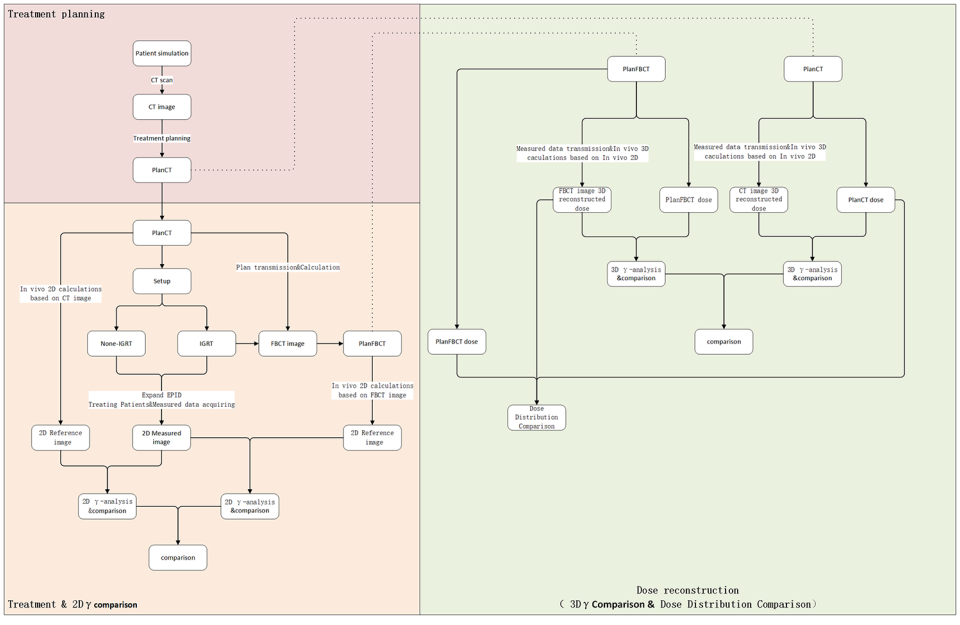

Fig. 1 Workflow for validating patient treatments in vivo. Note: illustrates the workflow for in vivo validation of patient doses. In this workflow, EPID (Electron Projectile Imaging Device) is utilized for in vivo dose verification, IGRT (Image-Guided Radiotherapy) is employed for precise treatment delivery, and FBCT (Fan-Beam Computed Tomography) is used for diagnostic imaging. Additionally, the in vivo dose verification includes both 2D assessment (in vivo 2D) and 3D reconstruction dose assessment (in vivo 3D) functions

for contouring. The delineation of target volumes encompasses the total tumor volume (GTVtb), which comprises all surgically implanted clips along with the solid tissue and/or seroma interspersed among them. The planned tumor volume (PGTVtb) is defined as a 1 cm extension of GTVtb, while the CTV encompasses the entirety of the affected breast. The planned target volume (PTV) is an exterior extension of 0.5 cm from the CTV, restricted to 0.5 cm beneath the skin, and the posterior margin does not encompass lung tissue. OAR includes the heart, left anterior descending coronary artery (LADCA) [17], affected lung, contralateral lung, liver, spinal cord, etc. The design uses a volumetric rotation intensity modulated plan (PlanCT for short) [18, 19]. The beam arrangement is divided into four 60°arc segments in both clockwise and counterclockwise directions (290°-350°and 100°-160°for the left breast, 10°-70 °and 200°-260°for the right breast), as shown in Fig. 2, the dose calculation grid is 2.5 mm, and the dose calculation algorithm used is the Monte Carlo algorithm. The prescribed dose for 25 fractions is PTV dose 50 Gy and PGTVtb dose 60 Gy [20]. The prescribed dose is normalized to PGTVtb 95% volume reaching 60 Gy. The medical physicist designs the treatment plan, Doctors and physicists evaluate the PlanCT, Treatment can only be carried out after the doctor's final approval. The target area evaluation index is PGTV D95 ≥ 60 Gy, PTV D95 ≥ 50 Gy. The limits of OAR include heart V5 < 30%, Dmean < 5 Gy, and lung V5 < 48%, V20 < 28%, and Dmean < 15 Gy. Before treatment, the PlanCT was validated using a 3D dose validation instrument MatriXX Evolution (IBA, Belgium), with a 3%3 mm pass rate of 99.23% ± 0.69%. At the same time, an in vivo 2D dose reference image based on PlanCT calculations, is produced.Plan information is detailed in Fig. 2.

(2) Patient Treatment: The linear accelerator system receives the PlanCT and treat the patient .Before and every week after the first treatment, patients need to use FBCT for image guidance in a state of free breathing, during which FBCT images can be obtained.Patients may have had position correction before treatment when they had a more than 5-mm shift according to our clinical protocol. For each therapy session, EPID was used to acquire doses in real-time. The criteria for the 2D γ-pass rate approach include a dose difference and distance to agreement (DTA) of 3% and 3 mm, respectively. The Gamma analysis threshold was set at 10%, with points below 10% of the maximum dose excluded. During the treatment, computed images from the planning system were compared with measured images obtained by EPID. The comparison utilized the in vivo 2D function, concentrating on user-selected arcs, to ascertain the 2Dγ-pass rate outcomes for the current arc.

(3) 3D Dose Reconstruction: In the retrospective analysis phase, 3D dose reconstruction is conducted. In our study, FBCT images used for IGRT were delineated by a senior radiotherapist for both the target area and OAR. Maintaining the parameters

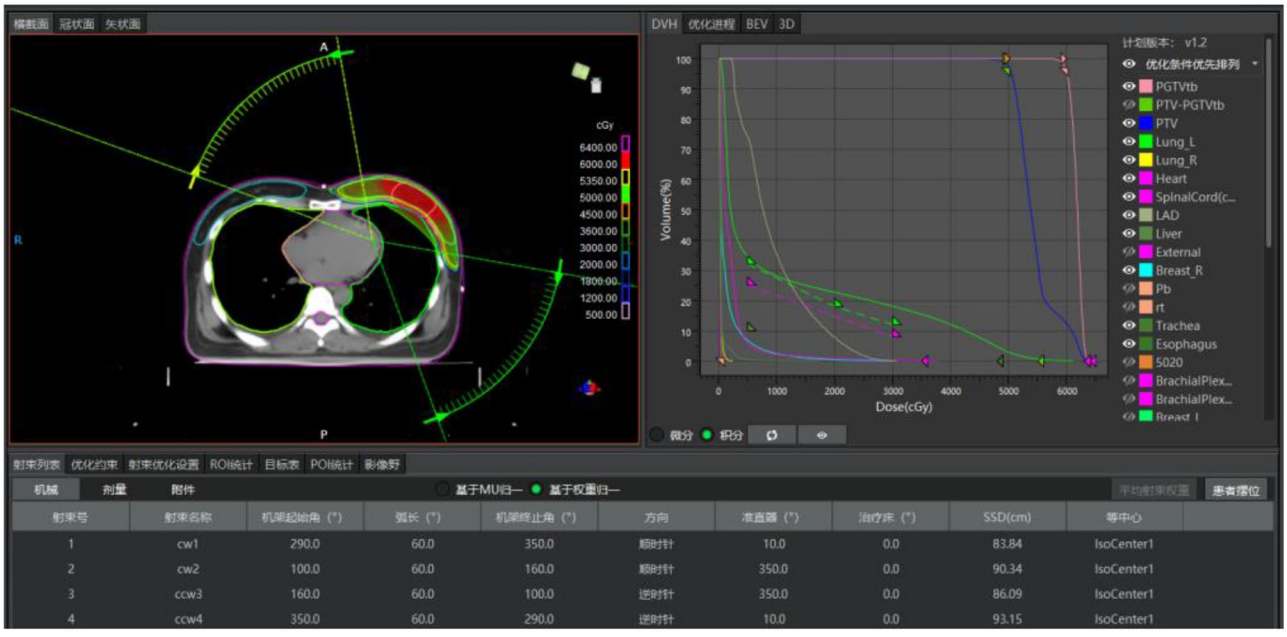

Fig. 2 Plan Information: Dose Distribution, DVH, Arc Segment Information

of the PlanCT (such as shot field arc segment, monitor units, subfields, etc.), the PlanCT data was transferred to the FBCT images to generate an FBCT image-based plan (referred to as the PlanFBCT). Then, using the in vivo 2D function, measured images based on FBCT were produced and contrasted with the reference images. Using the in vivo 3D capability, 3D dose reconstruction was performed on both the PlanCT images and FBCT images to compare 3D γ-pass rates and examine dosimetric differences.

Organs at Risk relative change and target area deformation analysis

Both CT images and FBCT images are based on the existing rigid registration relationship, and the overall contour is re drawn on the FBCT image to analyze the ROI and target deformation in more detail. Because in the OAR of breast cancer patients, the changes of heart and lung movement may be more obvious to the target area and the overall dose distribution. So these two organs were chosen as evaluation indicators.

Relative change in ROI (region of interest): We compared the ROIs designated for important organs (mainly the lungs and heart) on the FBCT images to those on the PlanCT images. The calculation used Eq. 1, which produced relative error values for the ROIs. A relative error value close to 0 indicates that the affected side lung and heart ROIs on the FBCT image closely match the PlanCT image.

$$\text{Relative error of } \mathrm{V_{ROI}} = \frac{\mathrm{V_i}}{\mathrm{V_0}} \times 100 \qquad (1)$$

where Vi refers to the ROI volume of the split FBCT images of the day; V0 refers to the ROI volume of the PlanCT images.

Target-area deformation evaluate: Drawing on the conformal index concept, we have proposed a deformation index for the Planning Target Volume (PTV) to characterize the disparity between the PTV of the FBCT image and that of the PlanCT image. In the current investigation, the PTV from the PlanCT image was replicated onto the FBCT image, and their intersection was generated utilizing a functional approach, as delineated in Eq. 2. The PTV deformation index is computed. The proximity of the PTV deformation index of the target area to 1 indicates that the FBCT picture closely approximates the volume of the target area in the intended image.

$$\text{Deformation index of } \mathrm{PTV_{CT}} = \frac{\left(\mathrm{PTV_{CT}} \cap \mathrm{PTV_{FBCT}}\right)^2}{\mathrm{PTV_{FBCT}} \times \mathrm{PTV_{CT}}} \qquad (2)$$

Where PTV-CT refers to the PTV outlined on the PlanCT image, and PTV-FBCT refers to the PTV copied on the FBCT image.

Comparison of in vivo dose validation pass rates

In the TG218 report, the planned pre-treatment validation evaluation was based on the gamma pass rate, which we also used for analysis. The 2D/3D γ-pass rate findings for all treatment fractions were consolidated into the ALL category. Treatment fractions without IGRT were classified into the N-IGRT group, while those with IGRT were assigned to the IGRT group. The ALL group, IGRT group, and N-IGRT group are analyzed and compared based on the reference images generated by PlanCT and the measured images generated by EPID. The reference images generated by PlanFBCT and the measured images generated by EPID are analyzed and compared to determine the FBCT group. The criteria for comparing the 2D/3Dγ-pass rates across these groups were set at 3%3 mm and 5%3 mm .

Comparison of dose distribution

Using the 2D in vivo measurement images obtained from EPID, a flux map is first reconstructed. Based on the flux map and the FBCT image of the day, the dose field received by the patient in vivo is reconstructed so that the actual dose distribution absorbed by the patient can be determined using in vivo 3D functionality. This procedure produces the patient's dose distribution based on the day's FBCT images, termed FBCT in vivo. Subsequently, this distribution was compared with the patient's PlanCT and the dose distribution of the PlanFBCT, respectively. For target areas, we counted PGTV D95, PGTV D2, PTV D95, and PTV D90; for critical organs, we counted Heart Dmean, V5, lung Dmean, V20, V5.

Statistical analysis

SPSS 19. 0 software was used to test all data for normality. In vivo, dose validation 2D/3Dγpass rate data is represented as the median and quartile values, denoted by [M (P25, P75)]. The Wilcoxon rank sum test was utilized for non-normally distributed data. A paired-design signed rank sum test was performed for data with identical sample sizes, but a grouped-design two-sample rank sum test was employed for data with varying sample sizes. A p-value of less than 0.05 was deemed statistically significant.

Results

IGRT could not completely correct the effect of posing errors on dose distribution

Both breast cancer patients experienced considerable displacement of the breast and diaphragm even after normal IGRT, shown in Fig. 3 (A, B, and C). The ensuing

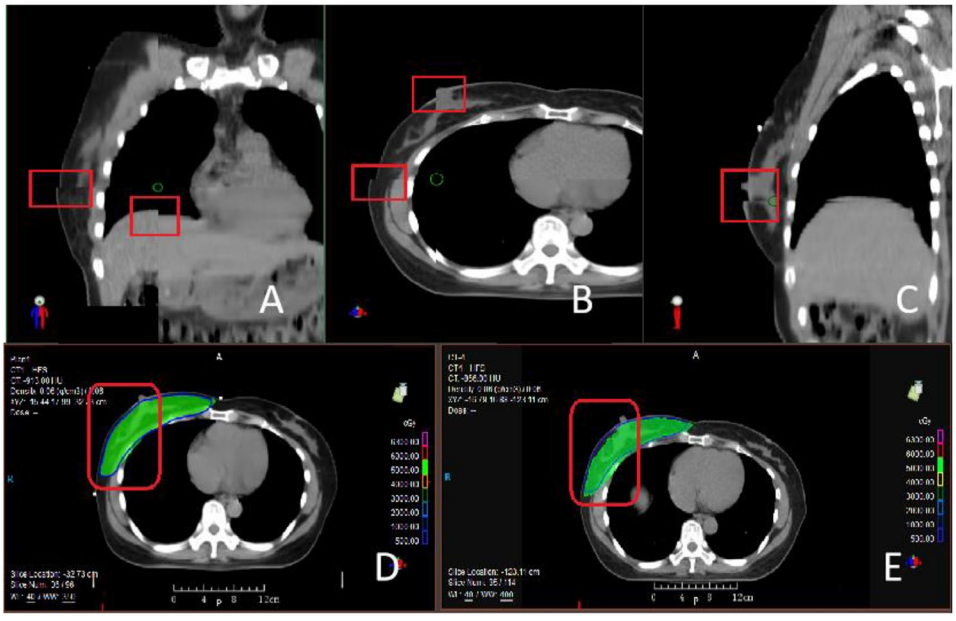

Fig. 3 For right breast cancer, the top row of images shows the positional deviation of the FBCT image and CT image fusion in coronal (**A**), transverse (**B**), and sagittal (**C**) planes on the same day, respectively

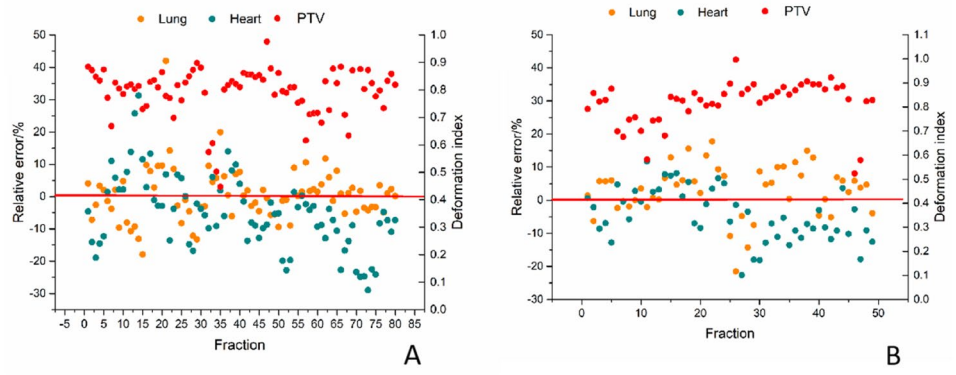

Fig. 4 Panel A displays the relative errors and PTV deformation indices of lung and heart volumes on the affected side for all IGRT subsets in patients with left breast cancer. Panel B presents the relative errors and PTV deformation indices of lung and heart volumes on the affected side for all IGRT subsets in patients with right breast cancer

under-dosage of dose in certain regions (highlighted in red boxes) due to positional aberrations can also be seen in Fig. 3(D, E).

The dosage distribution is depicted in the bottom row of photos, where D shows the dose distribution under the first planned CT scan, and E shows the actual dose distribution under FBCT imaging. The green area in the dose distribution pictures shows the 50 Gy-covered region.

The relative change of organs at Risk and target area deformation

PTV, lung, and heart analyses were conducted on FBCT images of breast cancer patients who underwent IGRT fractions, comprising 80 IGRT fractions for the left and 49 for the right. The relative errors of the lung and heart volumes on the affected side were computed for all IGRT-fractional FBCT images in left and right breast cancer cases utilizing Eq. 1. The deformation index of the PTV target area was calculated for all IGRT-fractional FBCT images in left/right breast cancer cases utilizing Eq. 2. Figure 4A presents the results for left breast cancer: the mean relative error of lung volume on the affected side was 0.57% ± 8.26%, with a maximum deviation of 42%; the mean relative error of heart volume was − 5.20% ± 11.44%, with a maximum deviation of 31.27%; the mean deformation index of the PTV target area was 0.80 ± 0.09, with a minimum value of 0.45. Figure 4B similarly presents the findings for right breast cancer: the mean relative error for lung volume on the affected side was 3.16% ± 7.72%, with a maximum deviation of -21.53%; the mean

relative error for heart volume was − 4.49% ± 7.95%, with a maximum deviation of -22.64%; the mean deformation index of the PTV target area was 0.82 ± 0.09, with a minimum value of 0.52.

In vivo dose verification γ pass rate results

There were 16 cases of left breast cancer, comprising 396 in vivo dose validations and 80 IGRT fractions during treatment. Among these, due to machine malfunction causing interruption during treatment, it is impossible to fully record the data of the day, the remaining 391 in vivo data points and 75 IGRT fractions were available for 3D analysis. Furthermore, there were 10 incidences of right breast cancer, accompanied by 247 occurrences of in vivo dose validation and 49 IGRT fractions throughout the treatment. For 3D analysis, the treatment range of a patient exceeded the monitoring range of in vivo dose, the remaining 223 in vivo data points and 44 IGRT fractions were available. The in vivo 2D/3D γ-pass rates were assessed using the PlanCT as the reference image and the same-day FBCT as the comparative image. The specific results are shown in Table 1.

Table 1 2D / 3D γ pass rates at different left and right breast cancer thresholds [M(P25, P75)]

		N-IGRT group(%)	IGRT group(%)	FBCT group(%)	All group(%)
left breast cancer	2D 3%/3 mm	88.51 (83.04, 92.41)	92.99 (90.86, 95.15)	93.32 (88.61, 97.46)	89.66 (84.28, 93.51)
	2D 5%/3 mm	93.87 (88.93, 96.31)	96.96 (95.29, 98.22)	98.02 (94.86, 99.38)	94.77 (90.03, 97.04)
	3D 3%/3 mm	89.53 (84.34, 93.18)	92.53 (88.34, 96.64)	93.93 (88.22, 96.80)	90.35 (85.08, 94.00)
	3D 5%/3 mm	95.38 (91.16, 97.81)	98.31 (94.15, 99.33)	98.84 (95.53, 99.54)	95.93 (91.84, 98.36)
right breast cancer	2D 3%/3 mm	87.49 (80.22, 91.86)	91.52 (86.00, 95.02)	92.03 (97.37, 96.13)	88.60 (82.46, 93.26)
	2D 5%/3 mm	92.69 (87.94, 96.33)	96.19 (92.88, 98.19)	97.35 (95.75, 98.68)	93.62 (89.13, 96.64)
	3D 3%/3 mm	85.39% (81.23, 90.44)	89.33 (86.44, 95.97)	92.21 (86.55, 96.49)	86.41 (82.02, 90.89)
	3D 5%/3 mm	92.26 (88.36, 96.23)	96.10 (93.87, 99.23)	98.54 (96.36, 99.41)	93.42 (89.66, 96.93)

Note: The N-IGRT group refers to the subset in which no image guidance was performed, Analyze theγpass rate of EPID and PlanCT; The IGRT group refers to the subset in which image guidance was performed, Analyze theγpass rate of EPID and PlanCT; The FBCT group refers to the subset in which the FBCT image of the same day was used as the reference image for comparison, Analyze theγpass rate of EPID and PlanFBCT, The All group:γpass rate analysis of N-IGRT group and IGRT group after integrating all data

As depicted in Fig. 5A and B in left breast cancer cases, the median of 3%3 mm 2D/3D and 5%3 mm 2D/3D in the IGRT group was higher than that of the corresponding N-IGRT group, and this difference was statistically significant ($p < 0.05$). Similarly, only 5%3 mm 2D/3D demonstrated statistical significance ($p < 0.05$), with the median of 3%3 mm 2D/3D and 5%3 mm 2D/3D in the FBCT group being greater than that of the matching IGRT group. Furthermore, there was a statistically significant difference ($p < 0.05$) between the IGRT group's median of 3%3 mm 2D/3D and 5%3 mm 2D/3D and the equivalent All group. The results of statistical analysis for right breast cancer cases (5 C and 5D)were consistent with those of left breast cancer cases.

In vivo dose validation dose distribution results

The dose distribution results of left and right breast PlanCT, PlanFBCT, and FBCT in vivo are shown in the Table (2).

Table 1 provides a detailed representation of PlanCT DVH, PlanFBCT DVH and FBCT in vivo DVH. In Tables 2 and 3, ΔDx /ΔVx1 represents the DVH difference between the PlanFBCT and PlanCT, primarily reflecting the dose distribution difference caused by inter-fractional differences. On the other hand, ΔDx /ΔVx2 signifies the DVH difference between the in vivo dose in vivo 3D and the PlanFBCT, predominantly indicating the dose distribution difference due to intra-fractional differences [14]. Tables 3 and 4 demonstrate that breast cancer radiation performed during free breathing displays inter- and intra-fractional variations, with intra-fractional variations having a more significant effect. As shown in Table 3, inter-fractional differences mainly affected the target area (PGTV D95, PGTV D2, PTV D95, PTV D90), heart (Dmean, V5), lung V5, with no significant differences observed for lung Dmean and V20; with the greatest effect on the heart at 8.21% ± 16.93%. Intra-fractional differences, except for heart Dmean, were significant for all the parameters; the actual heart V5 was biased by as much as 5%, and the target-area undershoot was relatively large at 3.39%. Taking the PTV D95 prescription dose of 50 Gy in the target area as an example, the inter-fractional difference resulted in an average underdose of 0.94 Gy. The intra-fractional difference resulted in an average underdose of 1.70 Gy. As depicted in Table 4, the inter-fractional difference in the target area mainly affected the target area, heart, and lungs V5, and there was no significant difference in lungs Dmean and V20. The maximum difference in the heart Dmean was 2.99% ± 7.26%. Intra-fractional discrepancies considerably affect all parameters in the target region, heart, and lungs, with the target area demonstrating a notable underdose of 3.66%, leading to varied levels of underdose for the other parameters (except V5). For

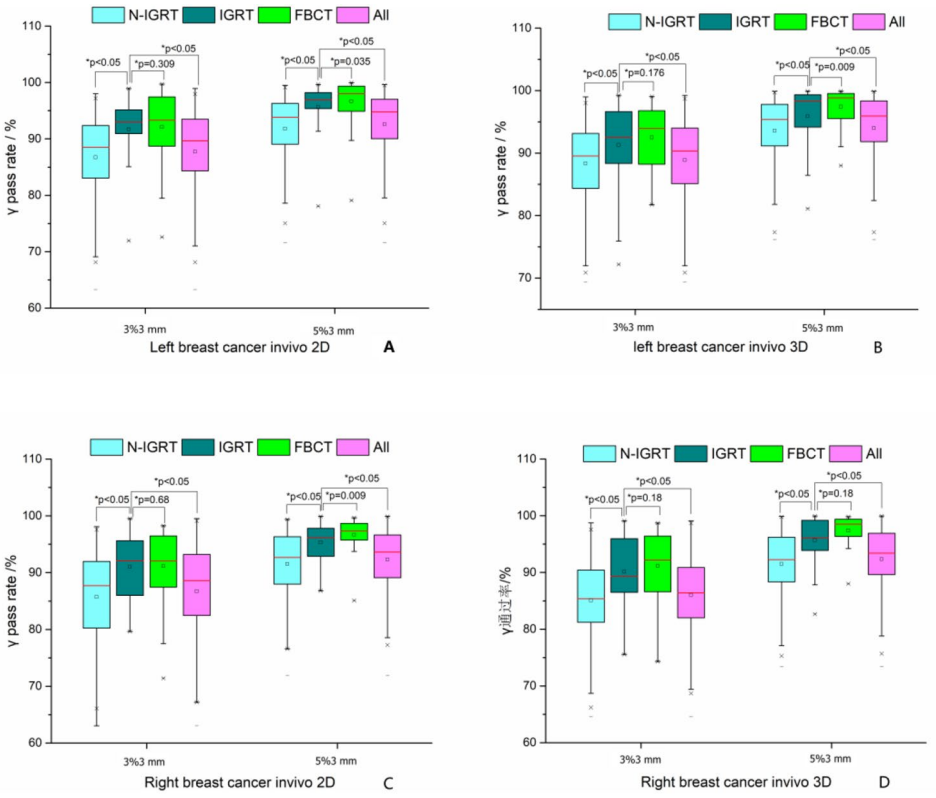

Fig. 5 Panels **A** and **B** display the results of in vivo dose-validated γ-pass rates for left breast cancer. Panel A represents in vivo 2D, while Panel B represents in vivo 3D. Similarly, Panels C and D depict the results of in vivo dose-validated γ-pass rates for right breast cancer. Panel C represents in vivo 2D, while Panel D represents in vivo 3D. The N-IGRT group refers to the subset in which no image guidance was performed, Analyze theγpass rate of EPID and PlanCT; The IGRT group refers to the subset in which image guidance was performed, Analyze theγpass rate of EPID and PlanCT; The FBCT group refers to the subset in which the FBCT image of the same day was used as the reference image for comparison, Analyze theγpass rate of EPID and PlanFBCT, The All group: γpass rate analysis of N-IGRT group and IGRT group after integrating all data

Table 2 DVH of left and right breast PlanCT, PlanFBCT, and FBCT in vivo

		PlanCT	PlanFBCT	FBCT in vivo			PlanCT	PlanFBCT	FBCT in vivo
Left	PGTV D95(Gy)	59.69 ± 0.47	59.95 ± 0.823	57.52 ± 1.38	right	PGTV D95(Gy)	59.73 ± 0.30	60.01 ± 0.60	57.94 ± 1.11
	PGTV D2(Gy)	63.89 ± 0.56	64.10 ± 0.78	63.65 ± 1.80		PGTV D2(Gy)	63.47 ± 0.53	63.85 ± 0.88	63.45 ± 1.46
	PTV D95(Gy)	50.78 ± 0.50	49.82 ± 1.12	48.13 ± 1.56		PTV D95(Gy)	50.75 ± 0.28	49.94 ± 0.99	48.15 ± 1.27
	PTV D90(Gy)	51.42 ± 0.53	51.02 ± 0.78	49.22 ± 1.41		PTV D90(Gy)	51.46 ± 0.29	51.09 ± 0.76	49.22 ± 1.19
	Heart Dmean (Gy)	4.28 ± 1.58	4.58 ± 1.65	4.57 ± 1.57		Heart Dmean (Gy)	0.87 ± 0.25	0.89 ± 0.24	0.86 ± 0.24
	Heart V5	19.45%±8.06%	20.64%±8.09%	21.36%±7.58%		Heart V5	1.04%±81.28%	0.86%±1.13%	0.89%±1.13%
	Lung Dmean (Gy)	10.28 ± 1.21	10.42 ± 1.32	10.16 ± 1.20		Lung Dmean (Gy)	10.27 ± 0.91	10.39 ± 1.15	9.96 ± 1.02
	Lung V20	18.70%±2.78%	18.97%±2.70%	18.72%±2.62%		Lung V20	19.89%±2.24%	20.11%±2.72%	19.43%±2.45%
	Lung V5	36.31%±4.16%	37.13%±4.897%	37.54%±4.53%		Lung V5	37.30%±3.35%	37.92%±3.97%	38.05%±3.86%

Note: PlanCT: DVH of PlanCT PlanFBCT: DVH of PlanFBCT

FBCT in vivo: in vivo DVH based on FBCT image reconstruction

example, considering the target area PTV D95 prescription dose of 50 Gy, inter-fractional differences lead to a mean underdose of 0.81 Gy. In comparison, Intra-fractional differences result in a mean underdose of 1.83 Gy.

Discussion

The breast tissue is near the lungs, and the chest wall experiences changes due to respiratory movement. This study revealed significant displacement of the breast, diaphragm, and other positions in 26 breast cancer patients undergoing radiotherapy after breast-conserving surgery despite the use of imaging guidance. This caused

Table 3 Results of PlanCT, PlanFBCT and in vivo DVH distribution in the left breast cance

Target & OAR		ΔDx /ΔVx1	ΔDx /ΔVx2	p-value	
				PlanCT vs. PlanFBCT	PlanFBCT vs. FBCT in vivo
Target	PGTV D95	0.45% ± 1.62	-4.04% ± 2.32%	< 0.05 (Z=-3.132c)	< 0.05 (Z=-7.324b)
	PGTV D2	0.32% ± 0.91%	-0.70% ±2.61%	< 0.05 (Z=-2.973b)	< 0.05 (Z=-2.171c)
	PTV D95	-1.88%± 1.96	-3.39%±2.46%	< 0.05 (Z=-6.355c)	< 0.05 (Z=-6.894c)
	PTV D90	-0.78% ±1.33	-3.53% ± 2.39%	< 0.05 (Z=-4.349c)	< 0.05 (Z=-7.081c)
Heart	Dmean	8.21%± 16.93%	0.57% ± 4.51%	< 0.05 (Z=-3.659b)	= 0.342 (Z = -0.951c)
	V5	8.15%±16.37%	5.08%±5.60%	< 0.05 (Z=-3.784b)	< 0.05 (Z=-5.170b)
Lung	Dmean	1.67% ± 8.74%	-2.32% ± 3.59%	= 0.235 (Z = -1.188b)	< 0.05 (Z=-5.407c)
	V5	2.21% ± 6.39%	1.27% ± 2.84%	< 0.05 (Z=-2.780b)	< 0.05 (Z=-3.712b)
	V20	2.19%± 11.01%	-1.24% ± 3.46%	= 0.329 (Z = -0.977b)	< 0.05 (Z=-4.924c)

Note: 1 denotes the variation in dose-volume histograms (DVH) between the current day's PlanFBCT and the PlanCT, reflecting inter-fractional variation; 2 denotes the variation in DVH between the on-treatment in vivo reconstruction dose and the current day's PlanFBCT, reflecting intra-fractional variation

Table 4 Results of PlanCT, PlanFBCT and in vivo DVH distribution in the right breast cancer

Target & OAR		**ΔDx /ΔVx1**	**ΔDx /ΔVx2**	***p*-value**	
				PlanCT vs. PlanFBCT	**PlanFBCT vs. FBCT in vivo**
Target	PGTV D95	0.49% ± 0.95	-3.52% ±1.59%	< 0.05 (Z=-3.700c)	< 0.05 (Z=-5.754b)
	PGTV D2	0.60% ± 0.91%	-0.69% ± 1.64%	< 0.05 (Z=-2.973b)	< 0.05 (Z=-2.282b)
	PTV D95	-1.62%± 1.79	-3.66%±1.47%	< 0.05 (Z=-4.843b)	< 0.05 (Z=-5.777b)
	PTV D90	-0.73%±1.20	-3.74% ± 1.52%	< 0.05 (Z=-3.565c)	< 0.05 (Z=-5.777b)
Heart	Dmean	2.99% ± 7.26%	-4.24%±5.17%	< 0.05 (Z=-2.002c)	< 0.05 (Z=-4.079b)
Lung	Dmean	1.27% ± 6.49%	-4.08% ± 2.74%	= 0.419 (Z = -0.809c)	< 0.05 (Z=-5.322b)
	V5	1.67% ± 3.72%	0.36% ± 1.84%	< 0.05 (Z=-32.597c)	< 0.05 (Z=-2.790c)
	V20	1.24% ± 7.38%	-3.26% ± 2.97%	= 0.397 (Z = -0.846c)	< 0.05 (Z=-5.310b)

Note: 1 represents the disparity in DVH between the current day's PlanFBCT and the PlanCT, signifying inter-fractional variation; 2 indicates the disparity in DVH between the on-treatment in vivo reconstruction dose and the current day's PlanFBCT, signifying intra-fractional variation

a disparity between the administered dose to the target region and the intended dose. This specifically manifested as a reduction in the γ-pass rate and underdose noted in the dosage distribution map. Literature reports suggest that respiratory movement can lead to a calculation error of 0.1% in the average cardiac dose, while errors due to positioning discrepancies can cause a 1.3% error in the calculated average cardiac dose [21]. Numerous factors, including the fixation mode [22, 23], arm posture [24], BMI [25], changes in psychological factors [26], and respiratory movement, can affect the morphology of the patient's body surface contour or organs during the entire radiation therapy process for breast cancer patients. Maintaining the same state as during localization is, therefore, complex. Thus, relying solely on image guidance is insufficient to correct this discrepancy. This study quantified the volumetric changes in the ROI across various inter-fractions using the relative error of the ROI volume change. The results showed that the multiple inter-fractions had notable variations in heart and lung volumes. In particular, the lungs' volume change was mostly within ± 20%. Because there is no respiratory motion management, photographs are acquired while breathing freely, capturing images with varying respiratory temporal phases over various fractions.

Consequently, this led to substantial changes in lung volume due to artifacts and other factors [27]. Furthermore, the volume of the heart exhibits more variability across different fractions than the lungs. In some instances, the volume of the heart is smaller during fractions than during localization. This phenomenon primarily arises from the rapid rhythmic movement of the heart and respiratory motion, which impacts the degree of volume change in the heart more significantly than in the lungs. Furthermore, if the first localization scan aligns with a specific cardiac motion phase, it may yield a bigger or smaller volume. Consequently, replicating this phase in successive fractions may prove challenging. Due to the unpredictable nature of the heart's rhythmic activity, it is prudent to contemplate relocation when the heart volume substantially exceeds that recorded during localization in several successive treatment sessions.

A related study [9] confirmed that errors in treatment could be identified through in vivo dose verification and the standardized utilization of this function could enhance its accuracy. Another study [28] indicated that errors in pendulum settings can significantly contribute to bias in γ-pass rates. In this investigation, the median of 3%3 mm and 5%3 mm 2D/3D in the IGRT group exceeded that of the corresponding N-IGRT group with statistical significance, suggesting that employing IGRT

can enhance the γ-pass rate of in vivo dose validation, consistent with the findings of Fen et al. [14]. Furthermore, the IGRT group's median 3%3 mm and 5%3 mm 2D/3D values were statistically significantly higher than those of the comparable ALL group, suggesting that improving the accuracy of the γ-pass rate can be achieved by altering the present weekly dose validation technique. This statistically significant difference implies that the γ-pass rate of in vivo dose verification in breast cancer cases can be improved by changing the current weekly image guiding mode and increasing the frequency of IGRT [20]. Thus, using the same day FBCT as the reference image can improve the 3%3 mm, 5%3 mm 2D/3D γ-pass rate for both right and left breast cancer, although only the 5%3 mm 2D/3D γ was statistically significant. The 3%3 mm threshold criterion may be excessively rigorous and could fail to identify substantial outcomes. Consequently, determining whether the decrease of the threshold criterion for γ analysis using FBCT images to implement the 5%3 mm criterion is more appropriate for clinical requirements necessitates further examination with a larger sample size [18, 29].

Some researchers [30] have suggested that 2D strategies have an advantage in rapid monitoring without requiring comprehensive data from all angles, but 3D methods give more specificity. However, the difficulty of 2D approaches to integrate with dose-volume histograms (DVH) is a limitation. The current study indicates a correlation between 2D/3D γ-pass rates, where a high 2D γ-pass rate corresponds to a high 3D γ-pass rate. Still, the correlation with the DVH of the 3D reconstruction is not robust, consistent with findings by Ma et al. [31]. The study found that the 3%3 mm γ-pass rate setting of 95% is too severe, as reported in the literature. The median 2D γ-pass rates were 92% for 3%3 mm γ-pass rates 97.2% for 5%3 mm γ-pass rates at IGRT, 89.2% for 3%3 mm γ-pass rates, and 94.5% for 5%3 mm γ-pass rates ungrouped [32]. Fewer research articles on EPID for Shanghai United Imaging Healthcare are present, even though the AAPM Task Group Report 307 [33] covers studies on in vivo dosage validation threshold settings for EPID currently used in the market [12.13.15].

Owing to the restricted data available, conclusive values cannot be ascertained, and additional research is necessary to enhance our comprehension of this domain. The ROI deformation data revealed a notable variance in the volumes of the lungs and heart across various fractions, indicating possible structural alterations that could affect the target area. These structural modifications may subsequently affect the dosage distribution within the target region. By comparing the dose distribution on the same-day FBCT for both left and right breast cancer cases with the planned initial dose distribution, it was observed that differences between fractions could affect parameters such as PGTV D95, PGTV D2, PTV D95, and PTV D90.

The present study observed small mean differences but large degrees of dispersion when comparing the dose distribution to the lungs for left and right breast cancer cases. Specifically, the standard deviations of affected side lungs Dmean, V5, and V20 were higher for left breast cancer (8.74%, 6.39%, and 11.01%, respectively) compared to right breast cancer (6.49%, 3.72%, and 7.38%, respectively). For the dose distribution of the heart, inter-fractional differences primarily affected the heart Dmean. The left breast cancer heart Dmean had the largest effect, with an overall deviation of 8.21% and an individual variation of 16.93%. In comparison, right breast cancer showed smaller variations within 3%, with an individual variation of 7.26%. This indicates that inter-fractional image discrepancies in the lungs and heart affect dose calculation results, as demonstrated by the greater dose variation in the affected lung side for left breast cancer relative to right breast cancer and the more significant dose difference for the heart in both right and left breast cancer compared to the lungs. This mismatch may be ascribed to the heart's main positioning on the left side of the chest, with its pulse influencing the volume of the left lung more significantly than that of the right lung in inter-fractional images [34].

Furthermore, differences in heart illumination and dose between right and left breast cancer cases contribute to smaller differences in heart Dmean on the right side. Considering the significant variation in heart and lung volume changes observed in this study, there appears to be some correlation between organ deformation and dose changes. Furthermore, increasing dosage dispersion indicates heightened randomness in the program outcomes, which may lead to misleading or overly optimistic expectations in program design and treatment evaluation. One study [35] demonstrated a 7.4% rise in the incidence of coronary heart disease for each 1 Gy increment in mean cardiac exposure [30]. The discrepancies in dose distribution between the heart and lungs in the original plan and the same-day FBCT indicate that IGRT alone is unable to fully rectify the dose variation received by mobile organs in different subsets of left/right breast cancer cases. This insight also guides the implementation of adaptive radiotherapy for breast cancer [36, 37].

To eliminate the influence of inter-fractional anatomical differences, we compared the results of in-vivo dose reconstruction with the PlanFBCT from the same day. In-vivo dose represents the actual dose received by the patient in real-time during treatment, focusing on analyzing the impact of intra-fractional anatomical variations on the dose distribution. Our findings, when examining cases of left and right breast cancers, revealed that intra-fractional differences significantly affected the

dose distribution within the target area, leading to an intra-target underdose (mean underdose of 3.39% for the left breast PTV D95 and 3.66% for the right breast PTV D95). Interestingly, intra-fractional differences had a more substantial impact on dose underdose in the target area compared to inter-fractional differences [12, 13] (left breast PTV D95 mean underdose 1.88%, right breast PTV D95 mean underdose 1.62%). Hence, the influence of intra-fractional organ motion on the actual dose should not be overlooked in clinical practice.

Intra-fractional differences also notably impact the dose distribution within the lungs and heart. Specifically, we observed elevated levels of low-dose regions, particularly evident in parameters such as V5 in the affected side lung (1.27% higher on average for left breast cancer and 0.36% higher on average for right breast cancer), V5 in the heart (5.08% higher on average). Dmean was 0.57% ± 4.51% higher in the heart for left breast cancer. Conversely, other parameters of the at-risk organs demonstrated varying degrees of reduction. Compared to inter-fractional data, intra-fractional differences in these parameters exhibited less variability across breast cancer cases. Additionally, while inter-fractional structural differences in lung and heart images significantly influenced dose alterations, intra-fractional organ motion had a comparatively lesser impact on these changes.

In summary, inter-fractional differences in breast cancer radiotherapy patients primarily manifest as changes in lung and heart volumes and their corresponding dose distributions. While IGRT can correct posing errors to some extent, it may not fully address these differences, highlighting the potential need for adaptive radiotherapy in breast cancer treatment. Intra-fractional variation, leading to inadequate coverage of the target area during treatment and reduced dose calculation accuracy for the lungs and heart, is primarily attributable to the absence of respiratory motion management in conventional breast cancer radiotherapy. Furthermore, related studies [38, 39] indicate that implementing respiratory exercises, including deep inhalation and breath-holding, can effectively displace the heart from the chest wall and enhance lung volume, consequently reducing radiation exposure to critical organs such as the heart and lungs. Incorporating radiotherapy techniques such as deep inhalation breath-holding may reduce intra-fraction variability and improve dose precision for patients undergoing breast-conserving radiotherapy.

There are some limitations in this study. One of the purposes of this study is to investigate the impact of inter- and intra-fractional variations on dose distribution. The relatively small size of the study sample restricts the extent to which the results can be generalized. Therefore, future research could involve larger cohorts, increasing the number of patients, and incorporating techniques such as deep inspiratory breath holding (DIBH) or adaptive radiotherapy to improve the accuracy and effectiveness of treatment and reduce potential adverse reactions.

Conclusion

The use of EPID-based in vivo dose validation in breast radiotherapy provides a practical approach for identifying and mitigating dose errors. By inter- and intra-fractional analysis, giving us a clearer understanding of the importance of inter- and intra-fractional variability. Strategies such as increasing the frequency of image guidance can identify and correct some of the problems in a timely manner, these measures enhance the accuracy of in vivo dose validation outcomes, ensuring that patients receive the prescribed radiation dose with precision. In conclusion, EPID-based in vivo dosage validation provides a precise real-time dose delivery evaluation for patients undergoing radiation therapy for breast cancer, Helping to enhance accuracy of radiotherapy and reduce the likelihood of side effects.

Abbreviations

IGRT	Image-guided radiotherapy
N-IGRT	Non-IGRT
FBCT	Fan beam CT
PTV	Planning target volume
CTV	Clinical target volume
GTVtb	Gross target volume tumor bed
PGTVtb	Planning gross target volume tumor bed
EPID	Electronic portal imaging device
IMRT	Intensity-modulated radiation therapy
ROI	Region of interest
DVH	Dose-volume histograms
BMI	Body Mass Index
DIBH	Deep inspiration breath-holding
DBCG	Danish Breast Cancer Cooperative Group
PGTV D95	Prescription dose covered by 95% of the volume of PGTV
PTV D95	The prescription dose covered by 95% of the PTV volume
D2	Maximum dose received within 2% PGTV volume
Heart V5	The percentage of volume contained in the heart receiving a 5 Gy dose
Lung V20	The percentage of volume contained in the lung receiving a dose of 20 Gy
Lung V5	The percentage of volume contained in the lung receiving a dose of 5 Gy
Dmean	Dose mean
PGTV D95 ≥ 60 Gy	The prescription dose of PGTV with 95% volume is ≥ 60 Gy
PTV D95 ≥ 50 Gy	95% volume of PTV prescription dose ≥ 50 Gy
Heart V5 < 30%	Volume percentage of heart receiving 5 Gy dose < 30%
Heart Dmean < 5 Gy	Heart dose mean < 5 Gy
Lung V20 < 28%	Volume percentage of lung receiving 20 Gy dose < 28%
Lung V5 < 48%	Volume percentage of lungs receiving 5 Gy dose < 48%
Lung Dmean < 15 Gy	Lung dose mean < 15 Gy
PTV D90	The prescription dose covered by 90% of the PTV volume
LADCA	Left anterior descending coronary artery
OAR	Organs at risk
UIH	United Imaging Healthcare
ASTRO	American Society for Radiation Oncology

Acknowledgements
Thanks to Chunyan Dai, Can Liao, Fei Zhao, Yu Wang, Zijie Mo, Xinmin Xu, Chuchu Wu, Yanyan Qiu, Yingjie Mei and Jiaqian Dai for their dedication.

Author contributions
WL Z, J F , SB D conceived of and designed the study. WL Z, J F performed literature search. Y Z, HZ Z, WL Z Conducted treatment and data collection, MC C Conducted Target area delineation, J F produce radiotherapy plans. WL Z, J F generated the figures and tables. WL Z, J F analyzed the data. WL Z wrote the manuscript. SB D critically reviewed the manuscript. WL Z, J F, SB D supervised the research. All of the authors read and approved the final manuscript.

Funding
Key Science and Technology Program of Jinhua City, Zhejiang Province (No. 2023-3-089). Jinhua Hospital affiliated with Zhejiang University School of Medicine Science and Technology Project (No.JY2021-1-02).

Data availability
Data sets used and/or analyzed during the current study are available from the corresponding author upon reasonable request.

Declarations

Ethics approval and informed consent to participate
This study in compliance with the Helsinki Declaration and has been approved by the Ethics Committee of Jinhua Hospital Affiliated to Zhejiang University School of Medicine (Approval Document Number: (Research) 2022480101). The subjects were aware of the study's purpose, risks, and benefits of this study and have signed an informed consent form.

Consent for publication
Not applicable.

Competing interests
The authors declare no competing interests.

Author details
[1]Department of Radiation Therapy, Affiliated Jinhua Hospital, Zhejiang University School of Medicine, Jinhua, China

Received: 29 April 2024 / Accepted: 2 January 2025
Published online: 11 April 2025

References

1. Radiation Oncology Physicians Branch of Chinese Medical Doctor Association. Guidelines for radiotherapy of breast cancer (Chinese Medical Doctor Association 2020 edition). Chin J Radiat Oncol. 2021;30(4):321–42. https://doi.org/10.3760/cma.j.cn113030-20210107-00010.
2. Mankinen M, Virén T, Seppälä J, Koivumäki T. Interfractional variation in whole-breast VMAT irradiation: a dosimetric study with complementary SGRT and CBCT patient setup. Radiat Oncol. 2024;19(1):21. https://doi.org/10.1186/s13014-024-02418-5. PMID: 38347554; PMCID: PMC10863193.
3. Hoekstra N, Habraken S, Swaak-Kragten A, Hoogeman M, Pignol JP. Intrafraction motion during partial breast irradiation depends on treatment time. Radiother Oncol. 2021;159:176–82. https://doi.org/10.1016/j.radonc.2021.03.029. Epub 2021 Mar 31. PMID: 33798609.
4. National Cancer Center/National Cancer Quality Control Center. Guidelines for the management of organ motion related to radiotherapy. Chin J Radiat Oncol. 2024;33(3):189–96. https://doi.org/10.3760/cma.j.cn113030-20230602-00149.
5. Han C, Schiffner DC, Schultheiss TE, Chen YJ, Liu A, Wong JY. Residual setup errors and dose variations with less-than-daily image guided patient setup in external beam radiotherapy for esophageal cancer. Radiother Oncol. 2012;102(2):309–14. Epub 2011 Aug 27. PMID: 21872956.
6. Reitz D, Carl G, Schönecker S, Pazos M, Freisledere P, Niyazi M, Ganswindt U, Alongi F, Reiner M, Belka C, Corradini S. Real-time intra-fraction motion management in breast cancer radiotherapy: analysis of 2028 treatment sessions. Radiat Oncol. 2018;13(1):128. https://doi.org/10.1186/s13014-018-1072-4. PMID: 30012156; PMCID: PMC6048710.
7. Kathpal M, Tinnel B, Sun K, Ninneman S, Malmer C, Wendt S, Buff S, Valentich D, Gossweiler M, Macdonald D. Deep inspiration breath hold with electromagnetic confirmation of chest wall position for adjuvant therapy of left-sided breast cancer: technique and accuracy. Pract Radiat Oncol 2016 Sep-Oct;6(5):e195–202. https://doi.org/10.1016/j.prro.2015.12.008. Epub 2016 Jan 4. PMID: 26922702.
8. Lee JJB, Lee IJ, Choi Y, Jeon MJ, Jung IH, Lee H. Clinical implications of geometric and dosimetric uncertainties of Inter- and Intra-fractional Movement during Volumetric Modulated Arc Therapy for breast Cancer patients. Cancers (Basel). 2021;13(7):1651. https://doi.org/10.3390/cancers13071651. PMID: 33916047; PMCID: PMC8036414.
9. Celi S, Costa E, Wessels C, Mazal A, Fourquet A, Francois P. EPID based in vivo dosimetry system: clinical experience and results. J Appl Clin Med Phys. 2016;17(3):262–76. https://doi.org/10.1120/jacmp.v17i3.6070. PMID: 27167283; PMCID: PMC5690938.
10. Mijnheer BJ, González P, Olaciregui-Ruiz I, Rozendaal RA, van Herk M, Mans A. Overview of 3-year experience with large-scale electronic portal imaging device-based 3-dimensional transit dosimetry. Pract Radiat Oncol. 2015 Nov-Dec;5(6):e679–87. Epub 2015 Jul 9. PMID: 26421834.
11. Fang J, Zhu WL, Dai CY, et al. Application of in vivo dose verification based on EPID in dynamic intensity modulated radiotherapy for lung and esophageal cancer.Chin. J Radiol Med Prot. 2023;43(9):705–11. https://doi.org/10.3760/cma.j.cn112271-20230316-00078.
12. Yu L, Zhao J, Zhang Z, et al. Commissioning of and preliminary experience with a new fully integrated computed tomography linac. J Appl Clin Med Phys. 2021;22(7):208–23. https://doi.org/10.1002/acm2.13313. Epub 2021 Jun 20.PMID: 34151504; PMCID: PMC8292712.
13. Chen L, Zhang Z, Yu L et al. A clinically relevant online patient QA solution with daily CT scans and EPID-based in vivodosimetry: a feasibility study on rectal cancer. PhysMed Biol. 2022;67(22). https://doi.org/10.1088/1361-6560/ac9950. PMID: 36220015.
14. Feng B, Yu L, Mo E, et al. Evaluation of Daily CT forEPID-Based transit in vivo Dosimetry. Front Oncol. 2021;11:782263doi. https://doi.org/10.3389/fonc.2021.782263. PMID: 34796120; PMCID: PMC8592931.
15. Jiang D, Cao Z, Wei Y, et al. Radiation dosimetry effect evaluation of a carbon fiber couch on novel uRT-linac506c accelerator. Sci Rep. 2021;11(1):13504. https://doi.org/10.1038/s41598-021-92836-2. PMID: 34188139; PMCID: PMC8242010.
16. Nielsen MH, Berg M, Pedersen AN, Danish Breast Cancer Cooperative Group Radiotherapy Committee. Delineation of target volumes and organs at risk in adjuvant radiotherapy of early breast cancer: national guidelines and contouring atlas by the Danish Breast Cancer Cooperative Group. Acta Oncol. 2013 ay;52(4):703 – 10. https://doi.org/10.3109/0284186X.2013.765064. Epub 2013 Feb 19. PMID: 23421926.
17. Feng M, Moran JM, Koelling T, et al. Development and validation of a heart atlas to study cardiac exposure to radiation following treatment for breast cancer. Int J Radiat Oncol Biol Phys. 2011;79(1):10–8. https://doi.org/10.1016/j.ijrobp.2009.10.058. Epub 2010 Apr 24. PMID: 20421148; PMCID: PMC2937165.
18. Piermattei A, Greco F, Grusio M, et al. .A validation study of adedicated software for an automated in vivo dosimetry control. Radiotherapy Med Biol Eng Comput. 2018;56(10):1939–47. https://doi.org/10.1007/s11517-018-1822-3. Epub 2018 Apr 23. PMID: 29682674.
19. Tang L, Ishikawa Y, Ito K, et al. Evaluation of DIBHand VMAT in Hypofractionated Radiotherapy for Left-sided breast cancers AfterBreast-Conserving surgery: a planning study. Technol Cancer Res Treat. 2021 Jan-Dec;20:15330338211048706. https://doi.org/10.1177/15330338211048706. PMID: 34657495; PMCID:PMC8521420.
20. Gradishar WJ, Moran MS, Abraham J et al. Breast Cancer, Version 3.2022, NCCN Clinical Practice Guidelines in Oncology. J Natl Compr Canc Netw. 2022;20(6):691–722. https://doi.org/10.6004/jnccn.2022.0030. PMID: 35714673.
21. Bai X, Wang B, Wang S, et al. Radiotherapy dose distribution prediction for breast cancer using deformable image registration. Biomed Eng Online. 2020;19(1):39. https://doi.org/10.1186/s12938-020-00783-2. PMID: 32471419; PMCID: PMC7260772.
22. Fang JH, Ma YJ, Shi JT et al. Comparison of imbolization accuracy between styrofoam and breast carrier in intensity-modulated radiotherapy after breast conservative surgery for breast cancer patients. Chin J Radiat Oncol 2019,28(5):369–72.https://doi.org/10.3760/cma.j.issn.1004-4221.2019.05.010
23. Ma MW, Wang SL, Qin SR, et al. Breast board combined with a thermoplastic head mask immobilization can improve the reproducibility of the treatment setup for breast cancer patients receiving whole breast and supraclavicular

nodal region irradiation. Chin J Radiat Oncol. 2019;28(3):217–21. https://doi.org/10.3760/cma.j.issn.1004-4221.2019.03.012.
24. Dekker J, Essers M, Verheij M, et al. Dose coverage and breath-hold analysis of breast cancer patients treated with surface-guided radiotherapy. Radiat Oncol. 2023;18(1):72. https://doi.org/10.1186/s13014-023-02261-0.
25. Song W. Li QS,Fu TX.Factors affecting the geometry variations of surgical clips in radiotherapy after breast-conserving surgery. Chin J Radiol Med Prot 2023,43(7):532–8.https://doi.org/10.3760/cma.j.cn112271-20230106-00005
26. Fidanzio A, Porcelli A, Azario L, et al. Quasi real time in vivodosimetry for VMAT. Med Phys. 2014;41:062103.
27. Sun ZW, Huang XY, Bao Y et al. Four-dimensional CT in the study of lung volume and respiratory movement. Chin J Radiat Oncol 2008,17(6):437–40.https://doi.org/10.3321/j.issn:1004-4221.2008.06.006
28. Kang SW, Li j,Ma JB et al. Evaluation of interfraction setup variations for post-mastectomy radiation therapy using EPID-based in vivo dosimetry. J Appl Clin Med Phys 2019,20(10):43–52.https://doi.org/10.1002/acm2.12712
29. Wu C, Hosier KE, Beck KE et al. On using 3D γ-analysis for IMRT and VMAT pretreatment plan QA. Med Phys. 2012;39(6):3051-9. https://doi.org/10.1118/1.4711755. PMID: 22755690.
30. Bresciani S, Poli M, Miranti A, et al. Comparison of two different EPID-Based solutions performing pretreatment Quality Assurance: 2D Portal Dosimetry Versus 3D Forward Projection Method. Phys Med. 2018;52:65–71. https://doi.org/10.1016/j.ejmp.2018.06.005.
31. Ma YG, Mai RZ, Pei YT, et al. The application and correlation study of γ rule and DVH evaluation for VMAT dose verification evaluation of cervical cancer patients. Chin J Radiat Oncol. 2022;31(5):450–5. https://doi.org/10.3760/cma.j.cn113030-20200927-00480.
32. Bossuyt E, Weytjens R, Nevens D, et al. Evaluation of automated pre-treatment and transit in-vivo dosimetry in radiotherapy using empirically determined parameters. Phys Imaging Radiat Oncol. 2020;16:113–29. https://doi.org/10.1016/j.phro.2020.09.011.
33. Dogan N, Mijnheer BJ, Padgett K et al. AAPM Task Group Report 307: use of EPIDs for patient-specific IMRT and VMAT QA.Med Phys,2023,50(8):e865–903. https://doi.org/10.1002/mp.16536
34. Yedekci Y, Biltekin F, Ozyigit G. Feasibility study of an electronic portal imaging based in vivo dose verification system for prostate stereotactic body radiotherapy. Phys Med. 2019;64:204–9. Epub 2019 Jul 24. PMID: 31515021.
35. Laugaard Lorenzen E, Christian Rehammar J, Jensen MB, et al. Radiation-induced risk of ischemic heart disease following breast cancer radiotherapy in Denmark, 1977–2005. Radiother Oncol. 2020;152:103–10. https://doi.org/10.1016/j.radonc.2020.08.007. Epub 2020 Aug 25. PMID: 32858067.
36. van Rooijen DC, van Wieringen N, Stippel G, et al. Dose-guided radiotherapy: potential benefit of online dose recalculation for stereotactic lung irradiation in patients with non-small-cell lung cancer. Int J Radiat Oncol Biol Phys. 2012;83(4):e557–62. https://doi.org/10.1016/j.ijrobp.2011.12.055. Epub 2012 May 23. PMID: 22632772.
37. Zegers CML, Baeza JA, van Elmpt W, et al. Three-dimensional dose evaluation in breast cancer patients to define decision criteria for adaptive radiotherapy. Acta Oncol. 2017;56(11):1487–94. Epub 2017 Aug 29. PMID: 28849731.
38. Lin A, Sharieff W, Juhasz J, et al. The benefit of deep inspiration breath hold: evaluating cardiac radiation exposure in patients after mastectomy and after breast-conserving surgery. Breast Cancer. 2017;24(1):86–91. Epub 2016 Feb 17. PMID: 26886584.
39. Zhao F, Lu ZJ, Yao GR et al. Application of deep inspiration breath hold in postoperative radiotherapy for left-side breast cancer.Chin. J Radiol Med Prot 2017,37(11):821–5.https://doi.org/10.3760/cma.j.issn.0254-5098.2017.11.004

Publisher's note